

# Experimental investigation of surface dielectric barrier discharge plasma actuator based on fluorinated polyimide

Dong-liang Bian<sup>a</sup>, Yun Wu<sup>b,\*</sup>

<sup>a</sup> Air Force Engineering University, 710038, Xi'an, China

<sup>b</sup> Xi'an Jiaotong University, 710049, Xi'an, China

## ARTICLE INFO

### Article history:

Received 17 December 2017  
Received in revised form 24 April 2018  
Accepted 24 April 2018  
Available online 27 April 2018

### Keywords:

Surface fluorination  
Plasma actuator  
SDBD  
Flow control

## ABSTRACT

In this paper, the mechanical performance, dielectric lifetime and material properties of the fluorinated polyimide (F-PI) based surface dielectric barrier discharge (SDBD) plasma actuator are studied and compared with a conventional polyimide (PI) based actuator. The results show that the force efficiency of the F-PI based actuator kept almost unchanged during 20 h of plasma discharge aging. Besides, dielectric lifetime of the F-PI based actuator was about three times as long as the PI based actuator at the applied sine voltage of 10 kV and frequency of 6 kHz. The scanning electron microscopy (SEM) images show that surface of the F-PI based actuator became more rough but kept integrated after aging, while that of the PI based actuator was severely etched by plasma. And the maximum surface temperature of the F-PI based actuator was about 18% lower than that of the PI based actuator. Furthermore, it was confirmed by X-ray photoelectron spectroscopy (XPS) that C–F and C–F<sub>n</sub> groups were incorporated onto the surface of the dielectric after fluorination, which was conducive to longer dielectric lifetime.

© 2018 Elsevier B.V. All rights reserved.

## 1. Introduction

Over the past decade, SDBD plasma actuators have been widely used in numerous flow control applications due to the ability to generate an electric wind in the boundary layer around various aerodynamic shapes [1–4]. They usually include two electrodes separated by a dielectric layer with one encapsulated and the other exposed to the open air [1]. Driven by sine wave voltage with frequency ranging from a few kHz to tens of kHz, surface-mode discharge will be generated from the side of the exposed electrode over the dielectric surface. The discharge directly transfers the momentum to neutral air by the collisions of energetic ions with neutral gas molecules and induces the ambient-gas motion along the surface to form the “ionic wind” [5]. In order to enhance the induced velocity or body force of the plasma actuators, the effects of parametric variations (e.g., exposed electrode shape [5–7], grounded electrode width [8,9], material permittivity [10,11], voltage waveform [12–14], etc.) and fabrication technology [15,16] on the performances of the actuators were studied widely, the performances have been optimized through changing geometrical and electrical parameters.

Despite the large number of literatures regarding how to improve the performance of the plasma actuators, few efforts have been made for their robustness. Due to joint advantages of high tensile strength, good thermal stability, chemical resistance and flexibility [17–19], layers of PI tape are commonly used as the barrier dielectric in SDBD plasma actuators [15]. However, it has been well acknowledged that polymers cannot withstand the intense bombardment of energetic active species, such as ions and electrons, which are emitted from plasma filaments [20–22]. In addition, the ultraviolet light and ozone which are generated from air SDBD plasma also have destructive effects on polymers [23–25]. Ndong et al. [26] and Hanson et al. [27] showed that degradation of PI based actuators was accompanied by an increase of consumed power. Pons et al. [20] found that two sorts of polymers (Poly methyl methacrylate and Polyvinyl chloride) degraded when exposed to 10 min of plasma operation in ambient air. Rigit et al. [28] found that plasma actuators manufactured from PCBs were visually shown to degrade and fail in some instances.

Since the dielectric degradation is unavoidable in polymer based SDBD plasma actuator, preprocessing of the dielectric needs to be done to enhance its robustness. As one of the most effective approaches to the chemical modification of polymer surfaces, direct fluorination using fluorine gas can obtain outstanding surface properties similar to the fluoropolymers. The research works and applications are mainly concentrated on improving dielectric

\* Corresponding author.

E-mail address: [biandl1990@163.com](mailto:biandl1990@163.com) (Y. Wu).

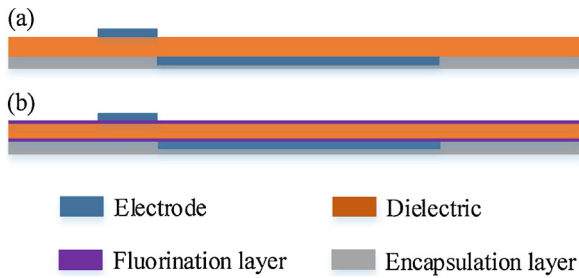


Fig. 1. PI based actuator (a) and F-PI based actuator (b). The schematic diagram is not according to the true scale.

properties, wettability, adhesiveness, chemical stability, biocompatibility and the electrical properties of polymers [29,30]. For example, An et al. [31,32] found that surface fluorination has a significant influence on charge injection and accumulation on the surface of the polyethylene. Du et al. [33] found that fluorination is an effective method for modulating the electrical properties and restraining the surface charge and space charge accumulation of the PI film.

The main goal of this study is to prolong the discharge lifetime of PI based SDBD plasma actuators. Thus, surface fluorination is used as a modification method of the dielectric. Firstly, the electrical properties were compared between the actuators with and without fluorination. Then, mechanical performance and dielectric lifetime were measured and evaluated. An in-depth study of surface morphology, surface temperature distribution and chemical composition were conducted to characterize the dielectric material properties and explain the degradation mechanism.

## 2. Plasma actuator and experimental set up

### 2.1. Plasma actuators

Dielectric barriers in this work were made of five-layer PI films. The top layer is pure PI film, while underlying four layers are PI films with silicone adhesive. The PI film has a thickness of 50  $\mu\text{m}$  and an area of 50  $\times$  50 mm. The dielectric strength and dielectric permittivity are 300 kV/mm and 3.4, respectively. Silicon adhesive has a thickness of 30  $\mu\text{m}$  and top temperature tolerance of 150°. The total thickness of the barrier dielectric is 0.37 mm. Before processing, the PI films were sterilized using alcohol, then rinsed with deionized water and ethanol using an ultrasonic cleaner. After cleaning, the films were dried in vacuum drying device. Surface fluorination of the dielectrics was carried out in a stainless reactor kettle with polytetrafluoroethylene lining at about 328 K (55°) using a  $\text{F}_2/\text{N}_2$  mixture with 20%  $\text{F}_2$  by volume [33]. Both the front and back sides of the barrier dielectric were fluorinated. After evacuation and purification with nitrogen gas more than three times, the reactive gas mixture was introduced slowly into the vessel until the mixture pressure in the vessel reached 0.05 MPa. The fluorination time was 60 min. After the treatment, the reactive gas mixture was purged from the vessel with nitrogen.

After surface fluorination, the electrodes were fabricated on the F-PI dielectric using ion beam sputtering technique. Cu was chosen as electrode material. The thickness of the exposed and encapsulated electrode was 200  $\pm$  5 nm. The width of the exposed and encapsulated electrode was 5 mm and 25 mm. There was no gap between two edges of two electrodes. Their effective span length (along which plasma was generated) was 30 mm. The encapsulated electrodes were covered in Kapton tape to prevent unwanted plasma formation. As shown in Fig. 1, the first actuator is denoted the PI based actuator (1#) and the second actuator is denoted the F-PI based actuator (2#) in present work.

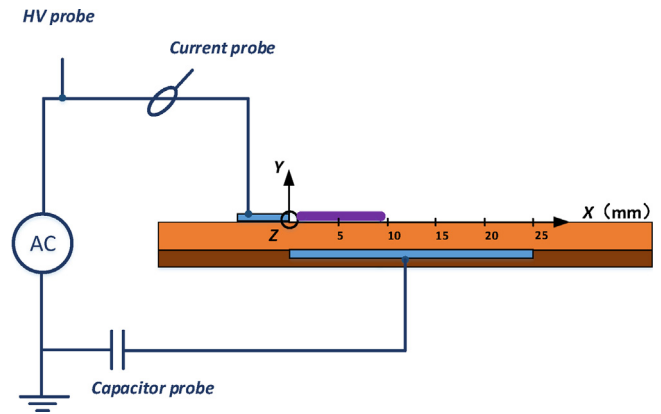


Fig. 2. Schematic diagram of the experimental set up.

### 2.2. Experimental set up

A SDBD plasma actuator test system is schematically shown in Fig. 2. A sinusoidal signal was generated using an AC power supply (CTP-2000 K). In this study, the plasma actuators were powered with two input parameters: 10 kV and 12 kV peak to peak voltage ( $V_{pp}$ ) with a fixed power frequency ( $f$ ) of 6 kHz. The applied voltage and discharge current were measured using a high voltage probe (Tektronix P6015A) and a current probe (Pearson 2100), respectively. Traces of the discharge voltage and current were displayed and recorded with an oscilloscope (Tektronix, DPO4014).

Measurement of the power consumption was conducted by integrating the charge-voltage ( $Q$ - $V$ ) cyclograms, as was earlier described in Ref. [8,27,34,35]. As shown in Fig. 2, a Class I ceramic capacitor was used as probe and placed between the encapsulated electrode and the ground, the capacitance ( $C_{pc}$ ) was measured by an impedance analyzer (Keysight E4990A) and the value was 10  $\pm$  0.01 nF at the frequency ranging from 1 kHz to 10 kHz. The voltage across the capacitor probe ( $V_{pc}$ ) was measured directly through an oscilloscope. The instantaneous charge,  $Q(t)$ , was the product of  $V_{pc}(t)$  and  $C_{pc}$ . The input voltage and charge values were plotted against each other to form closed curve, which was known as Lissajous figure. The area was equal to the consumed discharge energy per cycle ( $E_k$ ), which can be calculated by:

$$E_k = \oint_k C_{pc} V_{pc}(t) dV = \oint_k Q(t) dV \quad (1)$$

The consumed power  $P$  was the product of  $E_k$  and  $f$ :

$$P = fE = \frac{f}{K} \sum_{k=1}^K E_k \quad (2)$$

The corresponding standard deviation ( $\sigma_p$ ) was calculated by:

$$\sigma_p = \sqrt{\frac{1}{K-1} \sum_{k=1}^K \left[ \oint_k C_{pc} V_{pc}(t) dV - P \right]^2} \quad (3)$$

where Eq. (2) has already been averaged over  $K$  discharge cycles.

Additionally, Lissajous figure can also be utilized to analyze the discharge capacitance of the actuator [27,34]. As shown in Fig. 3, the capacitance was equal to  $dQ/dV$ . Two typical capacitance values were the cold capacitance ( $C_0$ ) and the effective capacitance ( $C_{eff}$ ), which occurred when plasma was absent and present, respectively. The calculation method of  $C_0$  and  $C_{eff}$  was based on a least squares fit of a straight line over the constant-slope regions, more details have been described in Ref. [27]. In this work, the valid data were filtered

Download English Version:

<https://daneshyari.com/en/article/7133392>

Download Persian Version:

<https://daneshyari.com/article/7133392>

[Daneshyari.com](https://daneshyari.com)